Characterization of Atmospheric Ammonia Emission from a Commercial Chicken House on the Delmarva Peninsula

5 AUTHORS, INCLUDING:

Ronald L. Siefert
United States Naval Academy

41 PUBLICATIONS **1,705** CITATIONS

SEE PROFILE

Joseph R Scudlark
University of Delaware

39 PUBLICATIONS **1,110** CITATIONS

SEE PROFILE

Kirsten Simonsen
National Oceanic and Atmospheric Administr…

7 PUBLICATIONS **45** CITATIONS

SEE PROFILE

Characterization of Atmospheric Ammonia Emissions from a Commercial Chicken House on the Delmarva Peninsula

RONALD L. SIEFERT,*,†
JOSEPH R. SCUDLARK,‡
AMELIA G. POTTER,§
KIRSTEN A. SIMONSEN,† AND
KAREN B. SAVIDGE‡

Chesapeake Biological Laboratory, University of Maryland Center for Environmental Science, 1 Williams Street, Solomons, Maryland 20688, Graduate College of Marine Studies, University of Delaware, Lewes, Delaware 19958, and Department of Natural Sciences, University of Maryland Eastern Shore, Princess Anne, Maryland 21853

A three-dimensional sampling grid using passive collectors was used to characterize the downwind gas-phase ammonia plumes originating from a commercial chicken house on the Delmarva Peninsula in the Chesapeake Bay watershed. Inverse Gaussian plume modeling was used to determine the source strength of the chicken house and the corresponding chicken emission factors. A total of seven field deployments were performed during two different flocks with a sampling duration ranging from 6 to 12.6 h. The deployments occurred during weeks 3, 4, and 5 of the 6-week chicken grow-out period in the months of May–July 2002. The ammonia emission factors ranged from 0.27 to 2.17 g of NH_3-N bird^{-1} day^{-1} with a mean of 1.18 g of NH_3-N bird^{-1} day^{-1}. Weighted emissions factors that accounted for the nonlinear increase in ammonia emissions over the 6-week grow-out period were also calculated and ranged from 0.14 to 1.65 g of NH_3-N bird^{-1} day^{-1} with a mean of 0.74 g of NH_3-N bird^{-1} day^{-1}. These weighted emission values would correspond to an annual release of approximately 18×10^6 kg of NH_3-N to the atmosphere from broiler production on the Delmarva Peninsula. This assumes that the emission factors in this study are representative for the entire year with varying meteorological conditions and are representative of all chicken husbandry practices. The Delmarva Peninsula could represent a significant source of nutrient nitrogen to the Chesapeake Bay and Delaware Bay watersheds through atmospheric deposition when considering the size of this annual release rate, the relative short atmospheric lifetime of ammonia due to deposition, and the proximity of the Delmarva Peninsula to the Chesapeake and Delaware Bays.

Introduction

Atmospheric deposition of nitrogen (N) species (ammonia and nitrate) is estimated to contribute 27% of the total nutrient N load to the Chesapeake Bay ([1]). Both wet and dry deposition contribute to this atmospheric deposition of nitrogen species. Castro and Driscoll ([1]) used the best available wet and dry deposition data from the National Atmospheric Deposition Program (NADP), the Clean Air Status and Trends Network (CASTNET), and the Atmospheric Integrated Monitoring Network (AIRMoN). However within these data sets, dry deposition data for particulate ammonium is scarce, and dry deposition data for gas-phase ammonia does not exist since gas-phase ammonia is not measured.

Ammonia is a multi-phasic atmospheric species that can occur in the gas phase (NH_3), in the particulate phase (NH_4^+), and in the aqueous phase (predominantly as NH_4^+). NH_x is defined as the sum of ammonia (NH_3) and ammonium (NH_4^+). There are large differences between the dry deposition rates of gas-phase NH_3 and particulate-phase NH_4^+ ([2]). These differences can lead to high deposition rates of gas-phase NH_3 near sources of gas-phase NH_3 ([2]). The conversion of gas-phase ammonia to particulate-phase NH_4^+ is dependent on the ambient concentrations of gas-phase and aerosol species (e.g., acids) and can impact the transport of ammonia. Because of this multi-phasic chemistry, NH_x has a relatively short atmospheric lifetime (hours to days) that is shorter than the atmospheric lifetime of nitrate or sulfate ([3]). Studies in Western Europe have shown that the transport and deposition is a complex process near agricultural sources ([4, 5]).

Current estimates of NH_x sources and deposition in the Chesapeake Bay airshed are not well constrained. A recent inventory for the Chesapeake Bay watershed indicates that agricultural livestock contribute 81% of the annual NH_x atmospheric burden ([6]). However, such estimates are derived from animal-specific emission factors ([7]), which are often based on many assumptions. Values for emission factors vary widely depending on the specific animal husbandry and manure dispersal practices utilized.

Annual broiler production on the Delmarva Peninsula, currently at 6×10^8 birds yr^{-1}, has increased more than 20-fold over the past two decades and has been cited for the 60% increase in NH_4^+ wet deposition observed nearby at Lewes, DE, during this time period ([8]). A primary concern when raising chickens in a confined space is the removal of elevated NH_3 inside the house by ventilation since NH_3 has adverse health effects on the chickens. Other functions of a ventilation system include the removal of heat, the removal of moisture (this may also decrease NH_3 volatilization by keeping the litter dry), and the provision of oxygen. Side-wall ventilation and tunnel ventilation are two common methods of ventilation. Direct NH_3 emissions from ventilating chicken houses contribute to NH_x emissions in the Chesapeake Bay airshed.

Previous studies have used different methods for measuring NH_3 emissions from agricultural buildings. Demmers et al. ([9]) used carbon monoxide as a tracer to determine the airflow rate through naturally ventilated livestock building while measuring NH_3 concentrations to determine the NH_3-emission factors for the livestock. Fowler et al. ([5]) measured NH_3 concentrations near a broiler house surrounded by woodlands and calculated that only 3.2% of the NH_3 emitted from the poultry unit was deposited within 230 m of the house and that 10% was deposited within 1000 m. Asman ([4]) predicted somewhat greater deposition over comparable distances, which is influenced by factors such as source height, wind speed, atmospheric stability, surface resistance, surface roughness, and plant NH_3 compensation point.
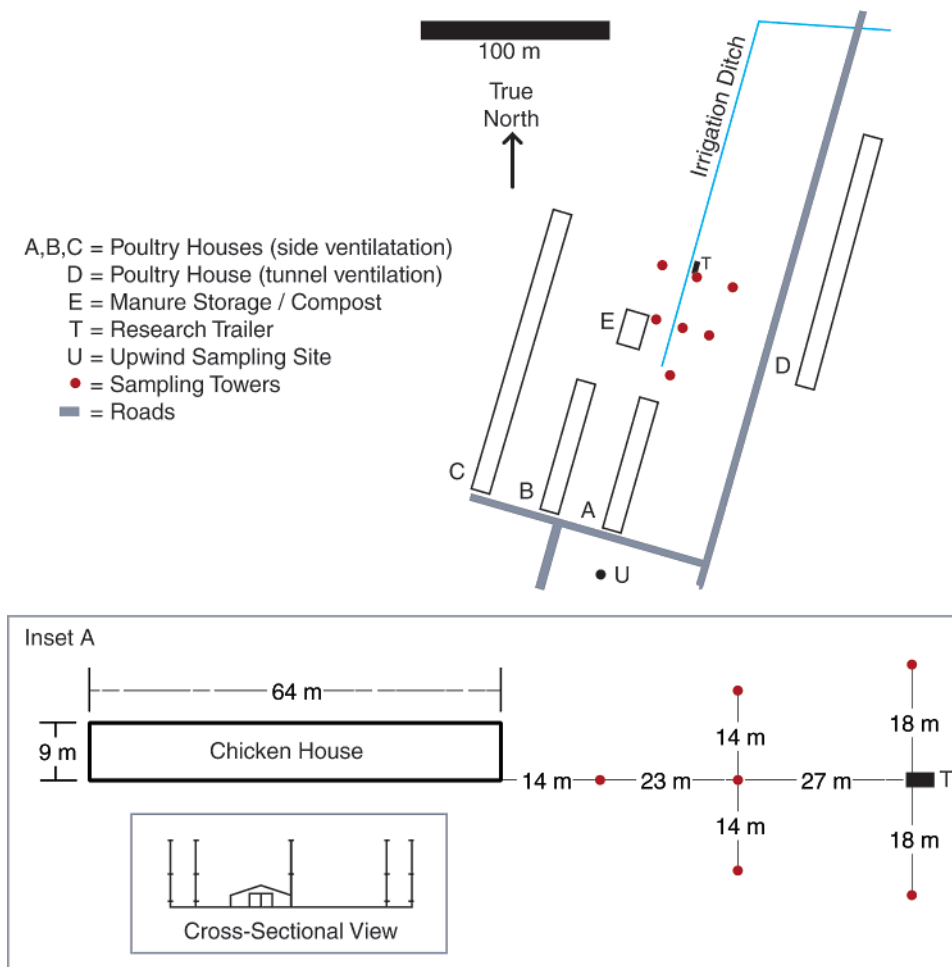
FIGURE 1. Map of farm with chicken houses and locations of sampling towers. Inset A provides more details about the arrangement of sampling towers and also shows the cross-sectional view of the sampling towers looking down the centerline of the chicken house.

The current estimates of the atmospheric deposition of ammonia/ammonium to the Chesapeake Bay and Delaware Bay are highly uncertain due to our limited understanding of the source strengths, atmospheric chemistry, and depositional processes for NH_x near strong sources. This study investigated NH_3 emissions from a side-wall ventilated commercial chicken house near Princess Anne, MD, on the Delmarva Peninsula. A three-dimensional sampling grid was used to measure the gas-phase NH_3 dispersion downwind of the 11 500 capacity chicken house. Inverse modeling of the NH_3 plume was performed to determine the ammonia source strength from the chicken house.

Methods

Ammonia Plume Sampling Downwind of the Chicken House. An array of 10 m high sampling towers was placed downwind of chicken house A to form a three-dimensional sampling grid (Figure 1). The arrangement of the towers was optimized for characterizing the NH_3 plume from the chicken house during SSW winds where the flow of air was parallel to the length of the chicken house. This arrangement was chosen in order to minimize the overlap of NH_3 plumes from the adjacent houses and also to minimize airflow disturbances due to the houses by minimizing the cross-sectional profile of the houses. The area has a flat topography, and the upwind and downwind areas have minimal trees and buildings. The field where the sampling was conducted was no-till planted with soybeans, which in May were just emerging and in July were at a height of about 30 cm A surface roughness length of 0.1 m was used for both the May and July study periods.

Passive gas-phase NH_3 samplers were located at heights of 1, 5, and 10 m on each sampling tower except at the research trailer location where samples were collected at only 1 and 5 m.

The tower arrangement and location heights of samplers were optimized by using a Gaussian plume model to predict downwind NH_3 concentrations (based on the number of birds in the house and published emission factors). The sampling grid was designed to be close enough to the source where sufficiently high NH_3 concentrations would allow a deployment time of about 6 h for the passive samplers. It was also advantageous to locate the sampling towers near the house to minimize the influence of the other nearby chicken houses. House B (Figure 1) was expected to influence concentrations in the sampling grid because of its proximity to house A. However house C and house D (a tunnel-ventilated house with the exhaust fan on the north end of the house) were far enough away from the sampling grid that they were not expected to influence the concentrations in the sampling grid. The sampling grid also needed to be located far enough from the source so that airflow disturbances due to the cross-sectional profile of the chicken house did not significantly impact the Gaussian plume profile (see inset A in Figure 1). An additional rationale for arranging the sampling grid at some distance from the chicken house is because it makes the influence of the source height on the concentration profile less important. The manure and compost shed (Figure 1) also could influence the airflow; however, the north and south ends of the building were open. Therefore it had a minimal cross-section during SSW winds. The manure and compost

shed could also influence NH_3 concentrations for the northwest sampling tower if the manure and compost had source strengths comparable to the chicken houses; however, no litter was being stored in the shed during this study. The accuracy of the vertical and horizontal dispersion coefficients used in the Gaussian plume model also decreases near the plume source (within roughly the first 50 m); therefore, it was better to sample further away from the house. Overall, the sampling design involved compromises between these competing considerations.

Meteorological Measurements. Meteorological measurements were performed at the research trailer location. A mast with an anemometer, wind vane, and temperature and relative humidity sensors was mounted above the research trailer. The overall height of the wind speed and wind direction sensors was approximately 6 m (about 3 m above the roof of the trailer on the upwind side of the trailer). The wind speed sensor had an accuracy of ± 0.5 m s^{-1}, and the wind direction sensor had an accuracy of $\pm 5°$ (Wind Sentry model 03001 anemometer and vane, Campbell Scientific, Inc.). The temperature sensor had an accuracy of ± 0.5 °C, and the relative humidity sensor had an accuracy of $\pm 3\%$ (model CS500 with a model 41301 6-plate radiation shield, Campbell Scientific, Inc.). Data acquisition was performed using a PC with a data acquisition card and LabView software (National Instruments, Inc.).

NH_3 Measurements. Ogawa passive samplers (Ogawa USA Inc., Pompano Beach, FL) were used to determine the time-averaged gas-phase NH_3 concentrations. Compared with traditional methods of NH_3 sampling (such as denuders), the passive samplers are ideally suited for this study since they are relatively inexpensive, robust, can be deployed unattended for extended periods, and do not require electricity.

The samplers were deployed using the rain shelter and clips provided by the manufacturer (see ogawausa.com). The rain shelter is required, even in the absence of rain, to minimize the effects of turbulence on the diffusive samplers as well as contamination from litter dust that is prevalent around the chicken houses. After deployment, the exposed samplers were sealed inside airtight plastic vials, and the vials were transported to the laboratory in an airtight plastic container and frozen until analysis. Filters from both ends of the passive sampler were combined for analysis in order to improve sensitivity, particularly during short deployments. Additional sampling details can be found in Roadman et al. (*10*).

Using stringent cleaning and handling protocols, the field blanks were 236 ± 112 ng of NH_3 ($n = 32$). For a typical 8-h deployment, this translates to an effective concentration of 15.8 μg of NH_3 m^{-3}, which represents less than 9% of the average observed concentration. On the basis of triplicate deployments at one location during each set of measurements, reproducibility averaged 7.6% at concentrations ranging from 46 to 505 μg of NH_3 m^{-3}.

Gaussian Plume Model. Lagrangian-based Gaussian plume models (GPMs) are commonly used to describe the dispersion of a species emitted from a point source (*11*). GPMs assume homogeneous horizontal and vertical turbulence and therefore are limited to specific idealized conditions. For example, vertical turbulence is not homogeneous, and the effect of this non-homogeneous vertical turbulence is more pronounced for sources near the ground due to the vertical wind velocity structure. However, the models are commonly used because of their simplicity, and in this study we have chosen a GPM to analyze concentrations profiles of NH_3 plumes emitted from commercial chicken houses. The error introduced by non-homogeneous vertical turbulence is also less pronounced in this study since the sampling array is located relatively close to the source.

An iterative computer program based on the GPM was used to determine the source strength of NH_3 from the chicken house for each of the field deployments. The GPM is referred to as an inverse GPM in this study since the GPM is being used to calculate the source strength based on the observed concentrations in the plume, as opposed to the usual use of a GPM to model the plume concentrations for a given source strength. The program was written using LabView software (National Instruments Inc., www.ni.com).

The chicken house was approximated as a line source in the model by using the principle of superposition to simulate the line source by incorporating multiple point sources along the length of the chicken house (*12*). The model was run using a horizontal grid resolution of 1 m; therefore, the distance between the point sources was 1 m. The length of the line source was allowed to vary in the model, but the end of the line source was always fixed at the north end of the chicken house. During the May/June study the exhaust fans were located along the length of the east side of the chicken house and therefore the line source was placed along the east side of the house. During the July study, the fans were arranged along the centerline of the house and were directed to blow the air toward the north end of the building where the north end doors were left open (see Figure 1, inset A); therefore, the line source was placed along the centerline of the house. The effective release height of the NH_3 was also allowed to vary in the model. The GPM also included chicken house B since this house could also influence the NH_3 concentrations on the west side of the sampling tower array. Again the principle of superposition was used to include this second chicken house in the model. Both chicken houses A and B were assumed to have identical emission characteristics in the model (e.g., source height, source length). This assumption was used since both chicken houses were identical in size and were operated identically (e.g., flocks arrived on the same date, similar feeding, similar ventilation).

The following GPM formula was used to generate the concentration profile for each point source:

$$\langle c(x,y,z) \rangle = \frac{q}{2\pi \bar{u} \sigma_y \sigma_z} \exp\left(-\frac{y^2}{2\sigma_y^2}\right)\left[\exp\left(-\frac{(z-h)^2}{2\sigma_z^2}\right) + \exp\left(-\frac{(z+h)^2}{2\sigma_z^2}\right)\right] \quad (1)$$

where c is the concentration (g m^{-3}), q is the source strength (g s^{-1}), x is the distance in x direction (m), y is the distance in y direction (m), z is the distance in vertical direction (m), σ_y is the horizontal dispersion coefficient (m), σ_z is the vertical dispersion coefficient (m), and h is the height of release (m). This formula is for total reflection at $z = 0$ (surface) and uses the slender plume approximation (*11*). The total reflection at the surface assumes that there is no significant deposition of gas-phase NH_3 in the sampling area. Under neutral conditions and with a source height of 3 m, Asman (*4*) showed that just over 20% of the NH_3 was deposited within 200 m of the source. These conditions would represent a conservative maximum since the field sampling in this study was closer to the source (within 120 m of the source). And Fowler et al. (*5*) observed only 3.2% of the total NH_3 being deposited within 230 m of a chicken farm surrounded by woodlands. The horizontal and vertical dispersion coefficients used in the Gaussian plume model were from Pasquill−Gifford correlations for different Pasquill stability classes (see ref *11*). These dispersion coefficients are a function of the downwind distance, x.

The concentration profile generated by eq 1 is for only one point source. The model included multiple concentration profiles that were generated using eq 1 and then superim-

TABLE 1. Summary of Conditions for Each Field Deployment (FD)

FD[a]	start date	description	study period (h)	flock age (d)	temperature mean ± SD[c] (°C)	RH mean ± SD[c] (%)	wind speed mean ± SD[c] (m s⁻¹)	wind vector direction (deg)	wind vector speed (m s⁻¹)	sky[e]	Pasquill stability date
I	May 31	afternoon	6.9	33	28.5 ± 1.1	58 ± 6	4.3 ± 1.2	193	4.11	CL	B, C
II	June 5	daylight	9.9	37	29.4 ± 1.4	62 ± 5	3.4 ± 1.1	180	3.02	CL	B, C
III	June 5	overnight	12.6	37	24.8 ± 0.7	80 ± 3	3.5 ± 1.3	186	3.32	CL	D
IV[d]	July 22	overnight	10.0	29	28.7 ± 1.9	62 ± 11	2.6[d] ± 1.7	187	2.42	CL, M	C
V	July 23	daylight	6.0	30	31.5 ± 0.8	54 ± 4	5.6 ± 1.4	193	5.35	OC	C
VI	July 27	afternoon	6.9	34	28.1 ± 1.0	76 ± 5	2.6 ± 1.4	184	2.42	OC, M	B
VII	July 27	overnight	12.0	34	23.6 ± 1.4	96 ± 4	0.1 ± 0.3	206	0.09	OC, M, F	NA[f]

[a] FD, field deployment. [b] The wind vector is the average wind vector over the duration of the deployment. Wind direction is relative to axis of the chicken house. For example, for a wind direction of 180°, the research trailer would be directly downwind of the chicken house. This corresponds to a true wind direction of 195° (SSW) since the chicken house makes an angle of 195 relative to true north. [c] SD, standard deviation. [d] There is missing data due to a power failure during deployment V. Therefore, the means and standard deviations are not for the entire deployment period. Weather data from Princess Anne indicated that the mean wind speed during the deployment was 3.5 m s⁻¹. [f] There is not a stability class defined for nighttime periods with wind speeds less than 2 m s⁻¹.

posed to model the chicken house as a line source and to also add the second chicken house (house B in Figure 1).

A cost function (CF) was defined to quantify how well the modeled concentrations compared to the measured NH_3 concentrations:

$$CF = \left(\frac{1}{j}\right) \sum_j \frac{(c_{\text{measured},i} - c_{\text{modeled},i})^2}{(2\sigma_{\text{measurement},i})^2} \qquad (2)$$

where $2\sigma_{\text{measurement}} = 2 \times$ standard deviation based on the accuracy of the atmospheric NH_3 measurements and j is the number of measurements. The program was written to sequentially vary each of the parameters (wind speed, wind direction, source length, source height, and source strength) until the program converged on a set of values that minimized the CF.

Confidence Limits on Source Strength. Two different approaches were used to estimate the confidence limits of the source strength from the inverse GPM. The first was to use the CF to determine how well the model concentrations compared to the actual measurement, and the second was to use a Monte Carlo simulation to quantify the variability of the inverse model in determining the NH_3 source strength.

The value of the CF is useful in quantifying how well the model compares to the measurements. The GPM accurately simulates the downwind dispersion of NH_3 from the chicken house, within the accuracy of the measurements, when the cost function is less than or equal to 1. This infers that, on average, the model concentrations are within the accuracy error of the NH_3 measurements. Values of the CF that are greater than 1 infer that the model concentrations are, on average, outside the accuracy error of the NH_3 measurements. For example, a value of the CF equal to 10 (using an estimated error for the measurements of ±10%) would correspond to the average difference between the modeled and measured NH_3 concentrations of 32%.

The model is an idealized simulation of the actual conditions, and values of the CF that are greater than 1 may be due to several reasons related to factors not accounted for by the GPM. Airflow disturbances due to structures are not accounted for in the model although the field site was chosen to minimize these effects. The model also simulates the chicken house as a line source; however, the chicken house is actually 9 m wide, and ventilation is on the sides of the building. The model also assumes that meteorological conditions do not vary over the deployment period; however, variations in wind speed and wind direction do occur during the sampling period even though the field sampling strategy attempted to choose sampling periods where these dynamics

were minimized. The model also assumes that the horizontal and vertical dispersion coefficients are accurate for this study site. Overall, all of these factors may contribute to higher values of the CF. However, it is difficult to ascertain a confidence limit on the source strength determined by the model by using the CF. A high CF may not necessarily mean that the source strength has high uncertainty but that the model assumptions are not accurate.

A Monte Carlo simulation was also performed to estimate the confidence limits on the source strength. Simulated data sets were generated for wind speed, wind direction, source height, and source length. The rejection method was used to generate normal (Gaussian) distributions of wind speed and wind direction (13). The manufacturer's stated accuracy for the sensors was used for the standard deviation of the wind speed (accuracy = ±0.5 m s⁻¹) and wind direction (accuracy = ±5°) for the simulated data sets. The reason for using the manufacturer's stated accuracy is because the GPM is based on the assumption that the wind vectors have a Gaussian distribution. This Gaussian distribution is the result of homogeneous turbulence and is the reason for the Gaussian-shaped plume. The source release height was a random height between 0 and 4 m (about the height of the chicken house). The source length was a random length between 11 and 64 m (the length of the chicken house) at 1-m intervals. Monte Carlo simulations were originally performed with random source lengths between 0 and 64 m; however, the results of these Monte Carlo simulations resulted in non-normal distributions. These Monte Carlo simulations were performed for each field deployment and represent the sensitivity of the source strength values with respect to the accuracy of the model inputs.

Results and Discussion

Field Deployments. Table 1 lists the seven field deployments (FDs) that were performed for this study. These FDs occurred during two different chicken flocks. The first three FDs were during the first flock, and the last four FDs were during the second flock. All of these FDs had durations between 6 and 12.6 h. The time to either deploy or retrieve the passive samplers was on average 40 min. The order in which the passive samplers were deployed and retrieved was the same for each FD.

Chicken House Operation and Field Conditions. Chickens were grown out for a 6-week period, and Table 1 includes the age of the flock for each field deployment. Chicken houses A and B both had approximately 11 500 chicks placed in the house at the same time, and approximately 11 150 were harvested (assuming a 3% mortality rate). Both chicken houses A and B had side-wall ventilation.
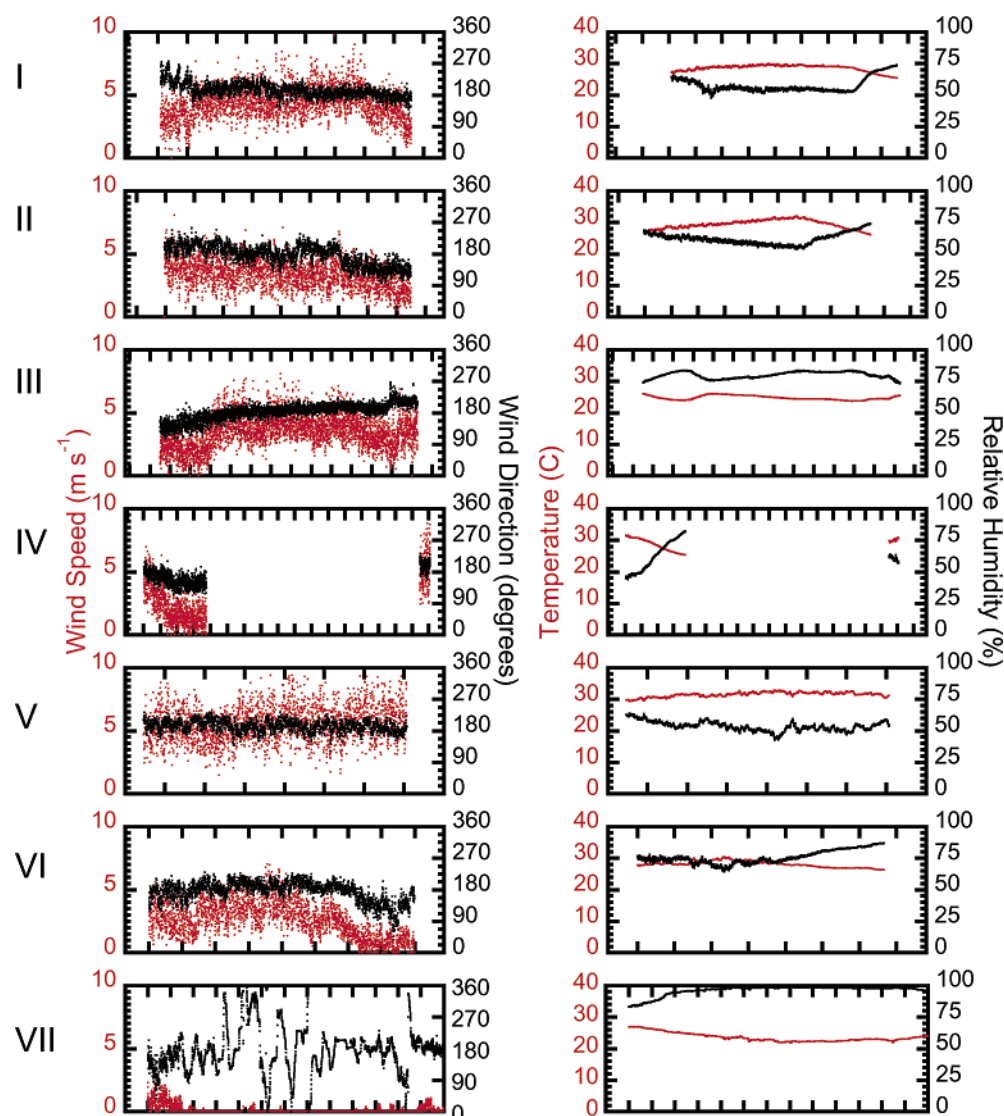
FIGURE 2. Meteorological conditions for each field sampling period (I−VII). One hour intervals are used for the inside tick marks on the *x*-axis.

Meteorology. Figure 2 shows the time−series measurements for wind speed, wind direction, temperature, and relative humidity for each FD. Table 1 lists the mean and averages for the meteorological measurements and also includes the sky conditions during the deployment periods (i.e., clear, mist, overcast, or fog) and the estimated Pasquill stability class (*11*). The wind direction in Figure 2 and Table 1 is relative to chicken house A (Figure 1), where a wind direction of 180° is parallel to the house (i.e., a SSW wind direction). Overall, the meteorological conditions (wind speed, wind direction, temperature, relative humidity) were relatively constant during each of the FDs. There is missing meteorological data for part of FD IV because of a power failure during the deployment period; however, the power failure did not effect the passive measurements. FDs I−VI had wind speeds that varied from 2.6 to 5.6 m s^{-1}, and FD VII had much lighter average winds (0.09 m s^{-1}) since it took place overnight under extremely calm conditions although the wind vector during this time period was still "in sector". FDs I, II, V, and VI took place during daylight hours; FDs III, IV, and VII occurred during nighttime hours. The concentration profiles measured in the FDs were use to determine the NH$_3$ source strength using inverse modeling.

Table 2 has wind frequency and direction distributions for locations with long-term meteorological observations and proximity to Princess Anne, MD, to determine the typical wind velocities and wind directions for the study site in Princess Anne, MD. These locations included Wilmington, DE (WDE: located 170 km N of site); Baltimore, MD (BMD: located 150 km NW of site); and Norfolk, VA (NVA: located 180 km SSW of site). Surface meteorological data (www.webmet.com) for the years 1961−1990 were used to generate frequency distributions using WRPLOT View software from Lakes Environmental Software (www.weblakes.com). Table 2 shows the frequency distributions for these locations and for the time periods relevant to this study.

The wind speed frequency distribution for the FDs in this study is also shown in Table 2, and the distribution is relatively close to the wind speed distributions for the nearby locations, although this study had a relatively small sampling (i.e., seven FDs). The temperatures during this study ranged from 23.6 to 31.5 °C. This range of temperatures is not very large but is consistent with the long-term temperature observations for the study period in nearby Salisbury, MD (20 km N of site). The long-term observations in Salisbury, MD, had mean temperatures, mean high temperatures, and mean low temperatures of 21, 27, and 14 °C for May 31−June 5 and 26, 31, and 20 °C for July 22−27. The mean yearly temperature is 13 °C, ranging from mean daily temperatures of 2 °C in

TABLE 2. Frequency Distributions for Wind Speed and Wind Direction for Nearby Loacations with Long-Term Meteorological Observations[a]

	wind speed (m s^{-1})							wind direction				
	<0.51 (%)	0.51—1.8 (%)	1.8—3.34 (%)	3.34—5.4 (%)	5.4—8.49 (%)	8.49—11.06 (%)	>11.06 (%)	SSE (%)	S (%)	SSW (%)	SW (%)	WSW (%)
				Time Period: May 31—June 5								
Wilmington, DE	5	3	35	38	18	1	0	5.7	8.6	6.0	8.5	9.3
Baltimore, MD	3	6	37	37	15	1	0	5.6	7.2	6.5	8.7	7.9
Norfolk, VA	2	3	21	41	30	3	0	5.2	10.4	11.2	13.9	7.0
				Time Period: July 22—27								
Wilmington, DE	8	4	36	37	15	0	0	6.8	10.2	6.3	8.2	6.8
Baltimore, MD	4	6	41	38	11	0	0	7.5	9.5	6.3	7.2	8.4
Norfolk, VA	3	6	27	41	22	1	0	5.4	10.0	10.1	11.9	7.5
				Time Period: May 31—July 27								
Wilmington, DE	6	4	38	36	16	1	0	6.5	10.0	6.3	8.6	8.5
Baltimore, MD	4	6	40	37	12	1	0	6.8	8.4	7.1	8.4	8.7
Norfolk, VA	4	4	24	40	25	2	0	5.4	10.6	12.0	14.1	6.8
				Time Period: May 31—July 27 (midnight to 6:00 am)								
Wilmington, DE	14	7	54	22	4	0	0	2.9	8.3	5.9	6.7	7.2
Baltimore, MD	9	11	54	22	3	0	0	3.0	6.5	5.9	8.4	10.0
Norfolk, VA	9	8	31	35	16	1	0	4.1	12.9	17.0	18.9	6.9
field deployments	14	0	29	43	14	0	0					

[a] The data sets used for each of the locations were from 1961 to 1990.

January and 25 °C in July. Overall, the temperatures during the study period were consistent with summer temperatures. Overall, the FDs in this study had wind speeds and temperatures that were representative of summer meteorological conditions in this region.

Concentration Profiles. Tables with the NH$_3$ concentration data for all of the FDs are included in the Supporting Information (see Supporting Information Tables 1−8). The mean downwind concentrations in the plumes ranged from 44.3 to 262 μg m^{-3} with concentrations from 22.1 to 1740 μg m^{-3} for all of the FDs. These concentrations are high relative to ambient NH$_x$ measurements in rural and urban areas around the Chesapeake Bay that are typically on the order of 1−3 μg m^{-3} (14). The concentrations in the plume are relatively low as compared to recommended exposure levels by the National Institute of Occupational Safety and Health (NIOSH) that recommend that workplace air should not exceed 25 ppm NH$_3$ (15 625 μg m^{-3}) over a 10-h workday or 40-h work week. The upwind NH$_3$ concentrations ranged from 0.2 to 59.8 μg m^{-3} with a mean of 16.7 μg m^{-3} for all the FDs (see Supporting Information Table 1). The maximum value of 59.8 μg m^{-3} was for FD VII during calm conditions. The upwind concentration was subtracted from all of the downwind plume concentrations for each FD since the GPM was for concentrations above the background concentrations.

The ratio of the maximum concentration to the minimum concentrations in the downwind sampling grid for each FD ranged from 18 to 60 except for FD VII, which had significantly less variability in the concentrations due to the meteorological conditions (see Supporting Information Table 1). The vertical NH$_3$ concentration profiles showed values that were typically higher nearer the surface for all of the FDs except for FD VII, which had lower concentrations near the surface. The concentrations profiles for FDs I−VII were consistent with a plume originating from the chicken house, and inverse GPMs were performed for these FDs to determine the source strengths.

Inverse Gaussian Plume Modeling. Table 3 lists the inverse GPM results for each the field deployments. The GPM varied wind speed, wind direction, house length, source height, and source strength until it minimized the cost function. The model was also run using different Pasquill stability classes, and the model run with the lowest CF is in boldface type in Table 3. Figure 3 shows an example of the

concentration density plots produced by the GPM for each of the sampling heights along with the corresponding observed gas-phase NH$_3$ concentrations for FD IV. The measured concentrations in Figure 3 have the upwind NH$_3$ concentration subtracted since the plume model is for NH$_3$ concentrations above the ambient (i.e., upwind) levels. FD IV was chosen as an example since it had a CF that was near the median of all the deployments. Both chicken houses A and B are included in Figure 3 since they are both included in the model calculations. Figure 3 clearly shows the strong vertical and horizontal gradients of NH$_3$ concentrations in the plume and is consistent with the measured NH$_3$ concentrations for this deployment. For example, the mast nearest the end of the chicken house had measured NH$_3$ concentrations (above background) ranging from 772 μg m^{-3} at 1 m to 55 μg m^{-3} at 10 m. Supporting Information Table 5 lists the associated CF for each of the sampling locations for FD IV (the average of this CF, 3.6, is given in Table 3).

The model consistently converged on values of wind speed and wind direction that were consistent with the mean wind speed and wind direction measurements considering the accuracy of these sensors (comparing Table 3 results in boldface type with Table 1 measurements). The model also converged on source release heights between 0.9 and 3.4 m that are consistent with the size of the chicken house for FDs I−VI. FD VII had a significantly higher source release height of 14.5 m. FD VII also had a vertical gradient with lower concentrations near the surface that was opposite of the vertical gradients observed for FDs I−VI. This high source release height for FD VII is probably do to the buoyancy of the ventilated air during the relatively calm and cooler overnight conditions during FD VII. The ventilated air had an estimated temperature of 30 °C as compared to the ambient temperature of 24 °C and would not have undergone as rapid of dilution as the previous FDs because of the relatively calm overnight conditions. The source height of 14.3 m would represent an effective source height. The effective source height is well above the highest sampling height (10 m). This buoyancy would also be a source of turbulence that could influence the dispersion of NH$_3$ that is not accounted for by the dispersion parameterization in the model. All of these factors probably contribute to the poor ability of the GPM to model the observations as indicated by the relatively high CF (27.0) for FD VII. The results are still

TABLE 3. Inverse Gaussian Plume Model Results To Determine the Ammonia Source Strength for Field Deployments I–VI[a]

FD[b]	stability class[c]	wind speed (m s⁻¹)	wind direction[d] (deg)	house start (m)	house length (m)	height of release (m)	cost function	source strength (g s⁻¹)
I	A	6.4	205	55	9	0.6	27.5	0.18
I	**B**	**3.9**	**187**	**36**	**28**	**3.0**	**13.7**	**0.13**
I	C	3.9	183	0	64	2.1	14.0	0.15
I	D	3.6	184	1	63	3.2	26.7	0.13
II	A	3.0	185	20	44	0.4	29.7	0.07
II	**B**	**2.8**	**176**	**25**	**39**	**1.7**	**1.8**	**0.11**
II	C	2.7	180	0	64	2.2	9.0	0.09
III	A	3.8	201	51	13	0.7	28.3	0.09
III	B	3.4	179	33	31	2.0	6.2	0.14
III	**C**	**3.4**	**180**	**0**	**64**	**1.4**	**6.0**	**0.15**
III	D	3.3	180	1	63	3.3	22.4	0.12
IV	A	2.9	181	8	56	0.4	22.4	0.24
IV	**B**	**2.8**	**182**	**3**	**61**	**0.9**	**3.6**	**0.25**
IV	C	2.5	187	0	64	3.2	13.4	0.15
V	A	6.2	186	23	41	0.6	25.9	0.22
V	**B**	**6.0**	**183**	**32**	**32**	**2.7**	**2.9**	**0.28**
V	C	6.0	184	0	64	2.8	8.8	0.25
VI	A	2.2	171	14	50	0.3	25.7	0.16
VI	**B**	**2.0**	**177**	**16**	**48**	**3.4**	**17.4**	**0.11**
VI	C	2.1	180	0	64	3.7	18.1	0.11
VII	A	0.3	201	61	3	16.0	39.9	0.028
VII	B	0.4	209	45	19	10.9	28.5	0.034
VII	**C**	**0.4**	**205**	**13**	**51**	**9.7**	**27.0**	**0.030**
VII	D	0.4	204	0	64	7.7	31.3	0.031

[a] The model was run using different Pasquill atmospheric stability classes for each run. The results in bold represent the model parameters that best fit the observations. [b] FD, field deployment. [c] The letters represent various Pasquill stability classes: A, extremely unstable; B, moderately unstable; C, slightly unstable; D, neutral. [d] Wind direction is relative to axis of the chicken house. For example, for a wind direction of 180°, the research trailer would be directly downwind of the chicken house.

presented in Tables 3 and 4; however, the confidence in the source strength value for this case is much lower than the other cases and difficult to quantify.

The length of the line source was allowed to vary in the model; however, the end source of the line source was always fixed at the north end of the chicken house. The length of the chicken house was obviously known; however, the reason for allowing the source length to vary was because the ventilation of the side-wall ventilated house was not well constrained. The model converged on source lengths between 28 and 64 m.

The GPM was also run for several atmospheric stability classes (see Table 3) to investigate if the model would converge to the estimated atmospheric stability class for each case (see Table 1) and to also investigate the sensitivity of the resulting source strengths for different stability classes (and therefore various dispersion coefficients). The Pasquill stability class was estimated for each hour during the sampling periods using an estimate for solar insolation (based on latitude, time of day, and cloud cover) and the wind speed (11). The GPM runs with the lowest CF agreed with the estimated Pasquill stability classes for FDs I, II, and VI. The GPM results for FD V converged on a Pasquill stability class of B although the predicted stability class was C. The GPM for FDs III and IV converged on stability classes one class higher (i.e., less stable) than the estimated classes. This higher stability class may reflect added turbulence (e.g., from the fans, wind direction changes, turbulence caused by the house's profile), which would increase the dispersion coefficients that is not accounted for by the meteorology. There was no definition of a stability class for the meteorological conditions observed for FD VII. The sensitivity of the stability class on the resulting source strength is shown in Table 3 by comparing the source strengths for each case. The average change in the source strength is 20% when changing the stability class to the next higher or lower stability class, and

the direction of that change was both positive and negative. The choice of stability class has a significant effect on the resulting source strength although a more rigorous sensitivity analysis is not possible since the stability class is not a continuous function. The use of another stability parameterization such as the Monin–Obukhov length would be a more useful parameterization to investigate the sensitivity of the atmospheric stability on the resulting source strength since this is a continuous parameter. For this study, however, the added insight of using this parameterization would not be very beneficial since more detailed atmospheric stability measurements would need to have been made during the study periods. The added uncertainties associated with the study site (e.g., house ventilation variability, turbulence around the building) and methodology (e.g., sampling several hours, accuracy of passive collectors) may also have limited the usefulness of a more detailed atmospheric stability parameterization. Overall, the ability of the model to converge on values that are consistent with the meteorological measurements gives some qualitative confidence in the source strengths generated by the inverse GPM.

The concentration profiles generated by the GPM were used to test the assumption in the GPM that no significant deposition occurs to the surface within the modeling (and sampling) domain. One method for estimating the dry deposition to the surface is to multiply the dry deposition velocity, by the area and the concentration at a reference height over the model domain, and then spreading this NH_3 deficit over the entire plume (ref 4 and references cited therein). The deposition of NH_3 was calculated for all of the GPM results by summing the deposition for each 1 m × 1 m grid point in the model domain. The total dry depositional flux for the sampling domain was investigated using a range of deposition velocities and using the NH_3 concentration at 1 m. For a depositional velocity (V_d) of 2 cm s⁻¹, the estimated total dry depositional flux to the surface outside of the house
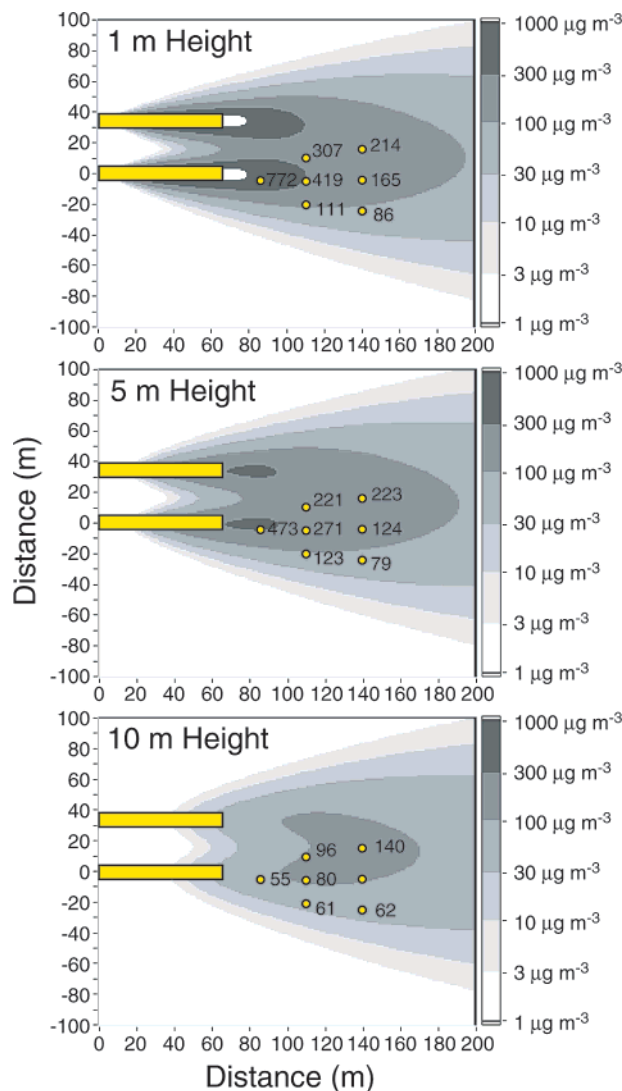
FIGURE 3. Ammonia concentration density plots generated by the Gaussian plume model for field deployment IV at the three height levels where the passive samplers were located. The two chicken houses are shown along with the location of the sampling towers and the corresponding measurements of gas-phase NH$_3$ concentrations (in µg m^{-3}).

It is difficult to determine relationships between the source strength values for the various deployments and the general conditions observed (e.g., meteorological conditions, chicken farm operation) due to the limited observations. The results seem to show that the source strengths were higher during July than late May/early June (omitting the anomalous FD VII). This may be due to different ventilation practices during these different times although the temperatures were very similar.

Table 4 summarizes the source strengths for each of the FDs and also lists the confidence limits for these source strength values based on Monte Carlo simulations. The source lengths used in the Monte Carlo simulations were a random number between 11 and 64 m, since including source lengths that were less than 11 m resulted in a non-normal distribution of source strengths for the Monte Carlo simulations. A short source length (≤10 m) resulted in a strong point source at the north end of the house that caused strong NH$_3$ gradients near the sampling locations; therefore, the inverse GPM converged on source strengths with anomaly high cost functions as compared to Monte Carlo simulations with source lengths between 11 and 64 m. Overall these source strengths represent atmospheric NH$_3$ emission rates from commercial side-wall ventilated chicken farms on the Delmarva Peninsula, using measurement of the actual plume concentration profile downwind of the chicken house. The sampling methodology and use of an inverse GPM show the ability of this combination to characterize sources of NH$_3$ from chicken houses.

Ammonia Emission Factors. Comparisons can be made using the source strengths determined in this study to previously published emission factors for chickens. Table 4 converts the NH$_3$ source strengths to NH$_3$ emission factors using a flock size of 11 155 birds for the chicken house used in this study (this assumes a 3% mortality rate). Table 4 also calculates a weighted emission factor using emission rate versus time data observed for a commercial chicken house in the U.K. (*15*). Demmers et al. (*15*) observed a strong nonlinear increase in NH$_3$ emissions as the birds age increased. The plot from Demmers et al. (*15*) of cumulative emissions versus time was used to determine the fraction of NH$_3$ emitted each day with respect to the total emissions and then used to weight the emission factors in Table 4. For example, it is estimated that 2.8% of the total emissions are released over the course of 1 day when the birds are 29 days

ranged from 2.9% to 8.7% of the entire source strength for all of concentration profiles produced by the GPM. This estimate is probably a maximum since the depositional flux near the surface would result in decreasing NH$_3$ concentrations near the surface and as a consequence a decrease in the depositional flux. The deposition velocity for this calculation is also probably high since the deposition velocity is generally lower than 2 cm s^{-1}. The inclusion of dry deposition to the GPM would lead to higher NH$_3$ emission rates from the chicken house since the dry deposition downwind of the house would result in an NH$_3$ sink and therefore there would need to be a higher emission rate from the chicken house to offset this NH$_3$ sink for a given NH$_3$ plume. The residuals (modeled − observed concentrations) also did not show any systematic trend of the modeled concentrations at the surface being lower that the other heights, which would be expected if there was significant dry deposition (the Supporting Information tables show the modeled and observed concentrations for each sampling location and case). Overall, the assumption that dry deposition within the model domain is not significant is a reasonable assumption for the cases in this study.

TABLE 5. Literature Values of NH₃ Emission Factors for Broilers

emission factor (g of NH$_3$-N bird^{-1} day^{-1})	ref
0.72	16
0.46	7
0.35	17
0.27	18
0.44[a]	10
0.80[b]	10

[a] Integrated over the entire grow-out period. [b] Last 2 weeks of grow-out period.

old. One day represents 1/42th (2.38%) of the entire grow-out period, so for FD V in Table 4, the emission factor of 1.94 g of NH$_3$-N bird^{-1} day^{-1} was multiplied by the ratio (0.0238/0.0280) to estimate the average emission factor over the entire 6-week grow-out period. Demmers et al. (15) also observed NH$_3$ released from the chicken house after the chickens had been removed but before the litter was removed. The weighted emission factors calculated in Table 4 do not take into account any NH$_3$ released from the litter after the chickens are removed from the house.

Table 5 lists NH$_3$ emission factors from several different literature sources. Overall, the literature values in Table 5 are on average lower than the NH$_3$ emission factors estimated by this study which had a mean of 1.18 g of NH$_3$-N bird^{-1} day^{-1}. The mean value of 1.18 g of NH$_3$-N bird^{-1} day^{-1} corresponds to 50 g of NH$_3$-N bird^{-1} released to the atmosphere during a 6-week grow-out period. Using the weighted emission factors in Table 4 results in a mean of 0.74 g of NH$_3$-N bird^{-1} day^{-1} that corresponds to 31 g of NH$_3$-N bird^{-1} released to the atmosphere during a 6-week grow-out period. Therefore the values in this study were about 1.5 times greater than these literature values when using the weighted emission factors.

The differences between the values from this study and the values in Table 5 may be due to several reasons. First, many of the values from Table 5 are from studies in Europe where different animal husbandry methods are applied to the raising of broilers. Also, because NH$_3$ emission rates are temperature-dependent, the values determined in this study during spring and summer (mean temperature range of 23.6–31.5 °C) might be expected to be greater than the European studies, where cooler temperatures typically prevail. The temperature and wind speed are also expected to be important meteorological factors that determine the NH$_3$ emission rates from chicken houses. There are many other factors (e.g., age of flock, litter moisture, diet) that are also important but are not directly related to the meteorology. Temperature is a factor that is important to the ventilation rate of the house. There is a minimal ventilation rate to keep NH$_3$ concentrations within the house below a level that is harmful to the birds, and as outside temperature increases, so does the ventilation rate to keep the birds cool (misters also may be used as the temperature increases). The release of NH$_3$ within the house (including the litter) may also increase with increasing temperatures. Wind speed may also effect NH$_3$ emission rates since winds may influence the ventilation rates of the chicken house especially for side-wall ventilated houses where winds directly contribute to the ventilation of the house. The effect of winds are probably less important for tunnel-ventilated houses where the fans dominate the ventilation rate.

The values from this study may also be higher because the birds in this study were near the end of their 6-week grow-out period for all of the FDs, although we attempted to correct for this by using a weighted emission factor (see above). Roadman et al. (10) investigated a tunnel-ventilated house on the Delmarva Peninsula and found an average NH$_3$ emission rate of 0.8 g of NH$_3$ bird^{-1} day^{-1} over the last 2 weeks of the grow-out period. This was about twice the rate integrated over the entire 6-week grow-out period and in closer agreement to the rates observed in this study.

Biases in this study may also be present since FDs to determine NH$_3$ emission rates were only performed when the wind direction was approximately from the SSW. The wind speed frequency distributions and temperatures were consistent with summer conditions for the seven study periods so the biases should be minimal for these factors. However waiting for winds from a certain sector may influence the results since these winds may be the result of certain meteorological systems that also bring distinct air masses. For example, NH$_3$ emitted from the house may undergo gas to particle conversion if the ambient air mass has acidic gas-phase and aerosol-phase species present. However, the concentrations of NH$_3$ close to the house where the sampling array is located are extremely high relative to typical atmospheric concentrations of NH$_3$ and other gas-phase and particulate-phase species that may react with NH$_3$. Overall, these interactions are probably not important within the plume where the sampling array was located but will become more important as the NH$_3$ is dispersed. The atmospheric deposition and lifetime of NH$_3$ will be effected if NH$_3$ undergoes gas to particle reactions.

Broiler Production on the Delmarva Peninsula and Implications for the Chesapeake and Delaware Bays. The source strengths determined by this study can be extrapolated to the entire Delmarva Peninsula. Approximately 587 000 000 broilers are produced annually on Peninsula (Delmarva Poultry Industry, Inc., www.dpichicken.org). Multiplying the annual broiler production by the weighted emission factor (31 g of NH$_3$-N bird^{-1}) yields an estimate of 18.2×10^6 kg of NH$_3$-N yr^{-1} emitted to the atmosphere from chicken houses on the Delmarva Peninsula. When compared with the current estimates of total atmospheric N deposition (nitrate + NH$_x$) to the Delaware (34×10^6 kg of N yr^{-1}) and Chesapeake Bay (177×10^6 kg of N yr^{-1}) watersheds (1) and assuming a sizable fraction of the local emissions are deposited locally, NH$_3$ emissions from poultry operations on just the Delmarva Peninsula would represent a significant additional contribution. Unfortunately, the current atmospheric deposition networks (NADP, CASTNET, AirMON) do not measure gas-phase NH$_3$ concentrations or deposition, thus it is impossible to gauge the relative contribution.

Supporting Information Available

Eight tables. This material is available free of charge via the Internet at http://pubs.acs.org.

Literature Cited

(1) Castro, M. S.; Driscoll, C. T. Atmospheric nitrogen deposition to estuaries in the mid-Atlantic and northeastern United States. *Environ. Sci. Technol.* **2002**, *36* (15), 3242−3249.

(2) Singles, R.; Sutton, M. A.; Weston, K. J. A multi-layer model to describe the atmospheric transport and deposition of ammonia in Great Britain. *Atmos. Environ.* **1998**, *32* (3), 393−399.

(3) Galperiin, M. V.; Sofiev, M. A. The long-range transport of ammonia and ammonium in the Northern Hemisphere. *Atmos. Environ.* **1998**, *32*, 373−380.

(4) Asman, W. A. H. Factors influencing local dry deposition of gases with special reference to ammonia. *Atmos. Environ.* **1998**, *32*, 415−421.

(5) Fowler, D.; et al. The mass budget of atmospheric ammonia in woodland withing 1 km of livestock buildings. *Environ. Pollut.* **1998**, *102*, 343−348.

(6) Chimka, C. T.; Galloway, J. N.; Cosby, B. J. *Ammonia and the Chesapeake Bay Airshed*; Scientific and Technical Advisory Committee of the Chesapeake Bay Program: 1997.

(7) Battye, R.; et al. *Development and Selection of Ammonia Emission Factors*; Office of Research and Development, U.S. EPA: Washington, DC, 1994.

(8) Scudlark, J. R.; Church, T. M. *A Comprehensive Re-Evaluation of the Input of Atmospheric Nitrogen to the Rehoboth and Indian River Estuaries*; Delaware Center for the Inland Bays: 1999; p 36.

(9) Demmers, T. G. M.; et al. First experiences with methods to measure ammonia emissions from naturally ventilated cattle buildings in the U.K. *Atmos. Environ.* **1998**, *32* (3), 285−293.

(10) Roadman, M. J.; et al. Validation of Ogawa passive samplers for the determination of gaseous ammonia concentrations in agricultural settings. *Atmos. Environ.* **2003**, *32*, 2317−2325.

(11) Seinfeld, J. H.; Pandis, S. N. *Atmospheric Chemistry and Physics: From Air Pollution to Climate Change*; John Wiley and Sons: New York, 1998.

(12) Fischer, H. B.; et al. *Mixing in Inland and Coastal Waters*; Academic Press: Orlando, FL, 1979.

(13) Press, W. H.; et al. *Numerical recipes in Fortran 77: The art of scientific computing*, 2nd ed.; Cambridge University Press: New York, 1992.

(14) Larsen, R. K.; Steinbacher, J. C.; Baker, J. E. Ammonia exchange between the atmosphere and the surface waters at two locations in the Chesapeake Bay. *Environ. Sci. Technol.* **2001**, *35* (24), 4731−4738.

(15) Demmers, T. G. M.; et al. Ammonia emissions from two mechanically ventilated UK livestock buildings. *Atmos. Environ.* **1999**, *33* (2), 217−227.

(16) Misselbrook, T. H.; et al. Ammonia emission factors for UK agriculture. *Atmos. Environ.* **2000**, *34* (6), 871−880.

(17) EEA. *Joint EMEP/CORINAIR Atmospheric Emission Inventory Guidebook*, 3rd ed.; European Environment Agency: Copenhagen, 2001.

(18) U.S. EPA. *Review of emission factors and methodologies to estimate ammonia emissions from animal waste handling*; U.S. EPA: Research Triangle Park, NC, 2002.